

Multishell Carrier Transport in Multiwalled Carbon Nanotubes

Saurabh Agrawal, Makala S. Raghuvver, Rampi Ramprasad, and Ganapathiraman Ramanath

Abstract—Understanding carrier transport in carbon nanotubes (CNTs) and their networks is important for harnessing CNTs for device applications. Here, we report multishell carrier transport in individual multiwalled CNTs, and films of randomly dispersed multiwalled CNTs, as a function of electric field and temperature. Electrical measurements and first-principles density functional theory calculations indicate transport across CNT shells. Intershell conduction occurs across an energy barrier range of 60–250 meV in individual CNTs, and ~ 60 meV in CNT networks. In both cases, the conductance behavior can be explained based upon field-enhanced carrier injection and defect-enhanced transport, as described by the Poole–Frenkel model.

Index Terms—Carbon nanotubes, electrical characteristics, multishell conduction.

I. INTRODUCTION

CARBON nanotubes (CNTs) are promising materials for nanodevice wiring due to ballistic carrier transport along the CNT axis arising from the unique molecular dimensions and structure. Metallic singlewalled CNTs of small diameters (e.g., 1–3 nm) would be the preferred solution over multiwalled CNTs which typically have larger diameters (e.g., 5–50 nm). But, the state of the art does not yet allow scalable separation or selective growth of metallic singlewalled CNTs in exclusion to semiconducting singlewalled CNTs. Hence, there is interest in exploring multiwalled CNTs as an alternative solution [1].

It is generally believed that charge carrier transport in multiwalled CNTs occurs primarily through the outermost shell [2]. The large diameters of multiwalled CNTs would ensure that even if the outermost shell is semiconducting (depending on chirality), the bandgap would be negligibly low (~ 1.5 meV for a 50-nm-diameter shell) to cause rectification [3]. Recent works have demonstrated the growth of aligned multiwalled CNT of controllable lengths in multiple predetermined orientations [4],

Manuscript received June 25, 2007. This work was supported in part by the National Science Foundation under Grant ECS 424322 and in part by New York State through the Focus Center. The work of G. Ramanath was supported by an Alexander von Humboldt Foundation Fellowship and by the U.S.–Israel Binational Science Foundation. The review of this paper was arranged by Associate Editor C. Zhou.

S. Agrawal, M. S. Raghuvver and G. Ramanath are with the Department of Materials Science and Engineering, Rensselaer Polytechnic Institute, Troy, NY 12180 USA (e-mail: ramanath@rpi.edu).

G. Ramanath was additionally affiliated with the Max Planck Institut für Festkörperforschung, Heisenbergstraße 1, 70569-Stuttgart, Germany.

R. Ramprasad is with the Department of Materials Science and Engineering & Institute of Materials Science, University of Connecticut, Storrs, CT 06269 USA.

Color versions of one or more of the figures in this paper are available online at <http://ieeexplore.ieee.org>.

Digital Object Identifier 10.1109/TNANO.2007.907798

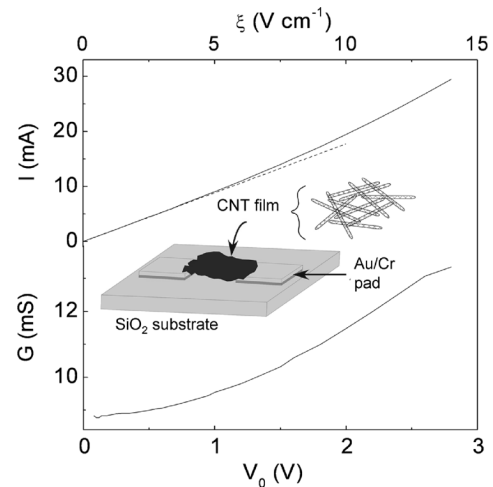


Fig. 1. Top graph showing room-temperature I - V_0 characteristics of a Au-contacted CNT network test structure (inset) showing super-linear behavior. Dashed line denotes extrapolation of the linear regime at $\xi < 5$ V cm $^{-1}$. Bottom plot shows differential conductance ($G = dI/dV$) plotted as a function of V_0 and ξ (top axis).

on a variety of substrates [5]–[7], and shown the proof-of-concept of using them as vertical interconnects in vias [8]. These attributes are advantageous for scalable device fabrication, and are yet to be realized in singlewalled CNTs. In order to fully evaluate the feasibility of using multiwalled CNTs for device applications, however, the electrical transport properties need to be more completely understood. Our findings reported here reveal that intershell carrier transport within each multiwalled CNTs, and across overlapping CNTs in networks, can significantly increase conductance. These features are not only interesting from a fundamental viewpoint, but also would be important considerations for designing CNT-based wiring and networks for device applications.

Charge transport along the CNT axis has been extensively studied, and reasonably well understood [9], [10]. Much less is known regarding the nature of carrier transport perpendicular to the axis in multiwalled CNTs [5], [11], [12]. Theoretical studies have predicted significant coupling between the 1-D electronic states associated with adjacent concentric graphene cylinders in multiwalled CNTs even in the absence of defects [13] due to the lack of electron wave confinement in a particular shell [14], [15]. Experimental verification has been impeded by difficulties in forming isolated electrical contacts between adjacent shells in the CNT. In a clever experiment, Collins and Avouris [16] obviated this difficulty by partially burning off the outer shell [17], [18] by current injection at selected locations, and formed contacts between adjacent shells. Their electrical measurements showing multiwalled CNT conduction even after removal of

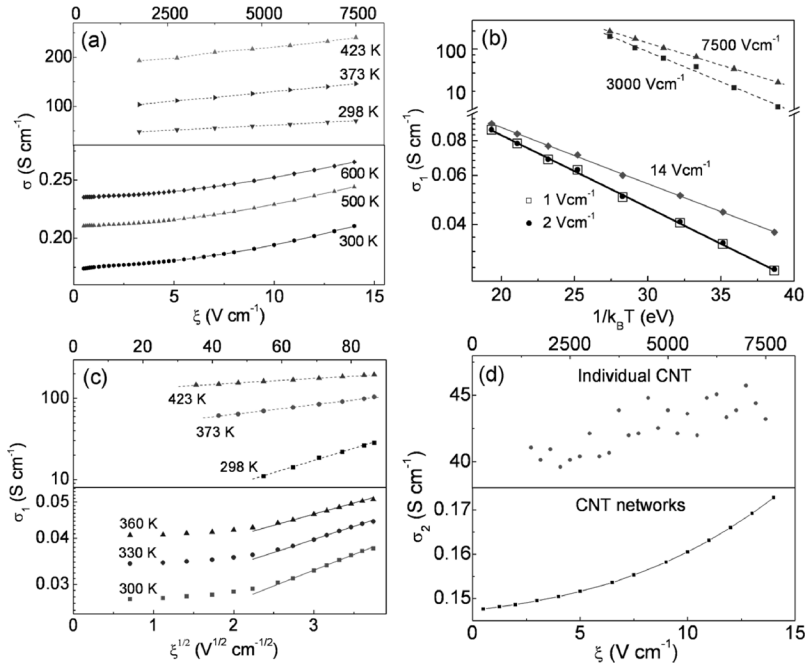


Fig. 2. Representative plots showing dependence of electrical conductivity σ on electrical field ξ and temperature T , for individual multiwalled CNTs (---), and films of CNT networks (—). (a) σ versus ξ at different T . (b) Semilog plot of σ_1 vs $1/k_B T$ for different ξ . (c) Semilog plots of σ_1 versus $\xi^{1/2}$ at different T . (d) σ_2 versus ξ showing super-linear behavior with $\sigma_2 \propto \xi^2$ in CNT networks. The upper curves in (a), (c), and (d) are referred with respect to the top axes.

more than ten shells revealed coupling between graphene shells. However, since the CNTs are damaged due to current injection and are likely to have defects that could significantly alter electrical transport, the exact nature of the coupling is not clear.

Recently we reported the existence of an energy barrier for thermally activated intershell conduction within each CNT, in individual multiwalled CNTs [19], and between neighboring CNTs in their random networks [20]. Similar behavior has been reported previously by other groups [21] in bundles of single-walled CNTs [22], [23], and c -axis conduction in graphite [24]. Here, we report a qualitatively similar behavior observed in mats of multiwalled CNTs, and reveal the effect of electric field on the energy barrier on carrier transport in individual multiwalled CNTs and their assemblies. We find that a significant component of the total conduction arises from thermally activated carrier hopping across a barrier at low fields, and field-assisted defect-mediated intershell carrier transport [20]–[23] at high electric fields, described by the Poole–Frenkel model. The presence of energy barrier is consistent with first principles density functional theory (DFT) calculations of double-walled tubes.

II. EXPERIMENTAL DETAILS

A 200-nm-thick Au film was deposited on an oxidized Si(001) substrate with a 650-nm-thick SiO₂ capping layer, and rectangular Au contact pads of dimensions $2 \times 2 \text{ mm}^2$ were carved using standard lithography and lift-off techniques. A 50-nm-thick interfacial layer of Cr was used in between Au and SiO₂ for enhancing adhesion. Multiwalled CNTs with diameters between 30 and 200 nm, prepared by standard arc-discharge technique, were dispersed in ethanol without sonication, and drop-coated to form a film consisting of randomly oriented CNTs over the Au pads (see Fig. 1 inset). The

electrode separation is 2 mm and the cross-sectional area of the CNT film for current flow is $\sim 1 \text{ mm}^2$. Contacts to individual multiwalled CNTs were formed by depositing Pt lines from PtCl₄ using a 30 keV focused ion beam. The ion dose on CNTs was limited to $\sim 2 \times 10^{16} \text{ cm}^{-2}$, which has been shown to be sufficient to create point defects in the shells without destroying CNTs with $> 50 \text{ nm}$ diameter [25]. These procedures ensure that the metal contacts are formed only to the outermost shells of the CNTs. Two-point-probe electrical measurements were carried out. The test devices were pretreated by heating in 10^{-7} torr vacuum to 650 K, to remove moisture and adsorbed gases. The electrical measurements were carried out at different temperatures between 300 and 600 K.

III. RESULTS AND DISCUSSION

Fig. 1 shows the room temperature electrical characteristics of a CNT network test structure. The nearly linear current-voltage (I - V) profile and a constant differential conductance ($G = dI/dV$) indicate ohmic behavior with a nominal resistance of 113Ω for nominal electric fields $\xi < 5 \text{ V cm}^{-1}$ obtained across the mm-spaced electrodes for voltages $V_0 < 1 \text{ V}$. The I - V characteristics become field-dependent at higher ξ , such that $G \propto |V_0|^{0.5}$. The I - V characteristics of individual multiwalled CNTs and their networks [see Fig. 2(a)] are similar to those reported earlier [16].

The conductivity of individual CNTs is about three to four orders of magnitude higher than the films of randomly dispersed CNTs presumably, suggesting that the intertube contact resistance in the latter samples is high. The net conductivity σ is a function of both ξ and T , and can be fit to the expression

$$\sigma(\xi, T) = \sigma_o \exp\left[-\frac{E_A}{k_B T}\right] + \sigma_2(\xi).$$

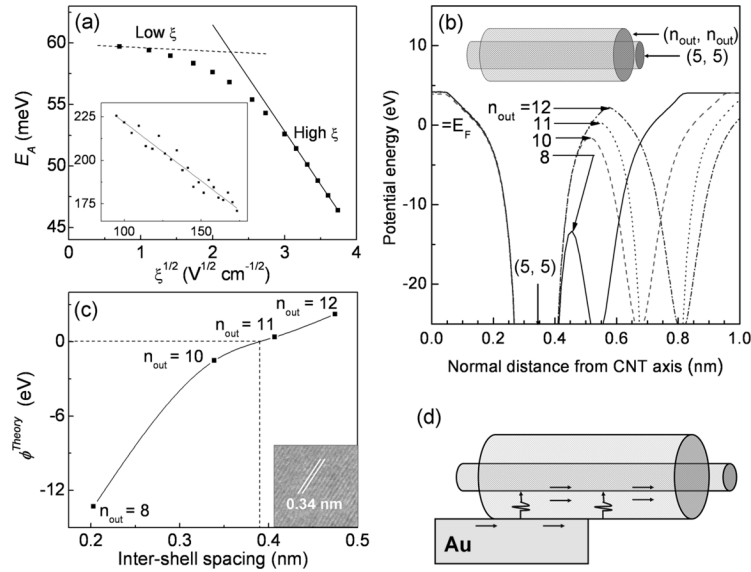


Fig. 3. (a) Activation energy E_A plotted as a function of $\xi^{1/2}$. The solid line captures the linear decrease in E_A at high ξ , while the dashed line denotes constant E_A at low ξ . Inset shows linear decrease in E_A with $\xi^{1/2}$ for a Pt-contacted individual multiwalled CNT. (b) The electron potential energy ϕ^{Theory} (referred to the Fermi Energy) in a double-walled CNT $(5,5)-(n_{\text{out}}, n_{\text{out}})$ plotted as a function of the perpendicular distance to the CNT axis. (c) ϕ^{Theory} plotted as a function of intershell spacing. The inset TEM micrograph from our multiwalled CNTs shows an intershell spacing of 0.34 nm. (d) Sketch illustrating multishell carrier transport. Carrier injection into the inner shells at high fields is depicted by the curved wiggled arrow.

where E_A denotes the activation energy for carrier transport. The two additive contributions represent parallel carrier transport pathways. The first term, designated as σ_1 , bears an Arrhenius dependence on temperature for both individual tubes as well as networks [see Fig. 2(b)]. We attribute E_A to intershell carrier transport. This designation is supported by our recent work demonstrating that shell crosslinking leads to $> 50\%$ decrease in E_A and threefold enhancement in electrical conductivity in individual multiwalled CNTs [19]. Additionally, E_A is a function of ξ for both sample configurations, as seen in Fig. 2(c) showing semilog plots of σ_1 with $\sqrt{\xi}$ at different temperatures. The electrical characteristics of networks for $\xi \sim 5\text{--}14\text{ Vcm}^{-1}$, and individual CNTs for $\xi > 1500\text{ Vcm}^{-1}$, are comparable. This difference in ξ range arises because the nominal ξ across the networks between mm-spaced electrodes is orders of magnitude lower than the localized electric fields expected across individual tubes and junctions.¹ Since individual shell conductivity starts to saturate [26] at $\xi \sim 2000\text{ Vcm}^{-1}$, similar to that used in our experiments over individual CNTs, our results showing continual conductance increase with increasing ξ suggests that σ_1 is due to contributions from field-assisted carrier injection into additional parallel conduction channels.

The temperature-independent second term σ_2 can be expressed as $\sigma_2 \propto \xi^\alpha$ where $\alpha = 2$ for CNT networks [see Fig. 2(d)], suggesting space-charge limited carrier transport that does not require thermal activation. The value of σ could not be estimated for individual CNTs due to the higher noise level in the data. The presence of nonthermally activated par-

allel conduction pathways is not surprising. Previously it has been observed that the barrier for conduction between two adjacent shells could be as small as 3 meV, causing nonthermally activated transport. In our samples, neighboring CNTs with outermost shells at atomic level proximity due to π - π stacking could cause nonthermally activated parallel transport. However, the barrier increases to ≥ 100 meV when conduction is over 10 shells deep [21].

For CNT networks, the variation of activation energy E_A as a function of $\sqrt{\xi}$ exhibits two different regimes [see Fig. 3(a)]. At low electric fields, $\xi < 5\text{ Vcm}^{-1}$, E_A is only weakly dependent on ξ and is characterized by $E_A|_{\text{low}\xi} \sim 60$ meV. At higher fields E_A decreases with ξ , and can be expressed as $E_A|_{\text{high}\xi} = \phi_0 - \beta\sqrt{\xi}$, where $\phi_0 \sim 80$ meV and $\beta \sim 1.38 \times 10^{-22}\text{ Jm}^{1/2}\text{ V}^{-1/2}$. We observe no systematic variation in E_A within ± 10 meV for different samples of networks, indicating that uncorrelated variations of the layout of the individual tubes in a large ensemble of randomly dispersed tubes do not have a major effect on the key electrical properties measured in our experiments. The high-field behavior is reminiscent of field-enhanced thermally activated charge transport described by the Poole-Frenkel model [27], [28], suggesting defect-assisted intershell hopping. Individual multiwalled CNTs also show a similar field-dependent behavior, i.e., $E_A|_{\text{high}\xi} = \phi_0 - \beta\sqrt{\xi}$, albeit with slightly higher activation energies in the 60–250 meV range [see inset in Fig. 3(a)] for $\xi \geq 1500\text{ Vcm}^{-1}$. The high noise levels in data obtained at lower fields (not shown) for individual tubes preclude the comparison of $E_A|_{\text{low}\xi}$ of individual CNTs with that of the networks.

The activation energy in CNT networks is 65 ± 5 meV in more than 10 samples studied, whereas individual multiwalled CNTs exhibit a much larger scatter from 70 to 250 meV. This difference is not surprising since the experimentally determined lower limit of E_A for the network represents the smallest barrier

¹Nevertheless, the use of the nominal field ξ to describe electrical transport in the networks is reasonable because ξ will affect the local fields across the individual nanotubes in networks, but it is difficult to measure the local fields directly. The use of nominal ξ for the networks is validated by the qualitative correspondence between the individual tubes data, and that of networks, and the similar activation energies at high fields.

amongst a range of inter-CNT spacings in the network, while individual CNTs with different diameters and defect structure would be expected to yield large variations in E_A . Joule heating is too small to account for the σ changes with increasing electric field. For example, even if we consider that the maximum heat generation rate (i.e., the total power input) for the highest voltage used in our experiments is balanced solely by thermal conduction along the CNT length, the temperature increase $\Delta T < 1 \text{ K}^2$. Inclusion of other heat dissipation mechanisms, e.g., radiation, convection, and heat transport to the substrate, would make ΔT even smaller.

First principles density functional theory (DFT) calculations confirm the validity of our attribution of E_A to intershell carrier transport. We determined the potential energy perpendicular to the CNT axis for double-walled CNTs composed of two concentric armchair (n,n) metallic shells: a (5,5) inner tube and different outer shells of $n_{\text{out}} = 8, 10, 11, \text{ and } 12$. Armchair shells serve as valid analogues that qualitatively mimic the two outermost shells of the 30–50-nm multiwalled CNTs investigated experimentally because the latter can be either metallic or semiconducting with negligibly small bandgap ($\sim \text{few meV}$). The results [Fig. 3(b)] reveal the minimum energy intershell barriers ϕ^{Theory} as a function of intershell lattice spacing. For $\phi^{\text{Theory}} = 60 - 250 \text{ meV}$ the intershell spacing is $\sim 0.39 \text{ nm}$, which is within 15% of the experimentally measured value of $0.34 \pm 0.01 \text{ nm}$ by TEM [see Fig. 3(c)], supporting the validity of E_A attribution to intershell transport. In light of the several simplifying assumptions made to render the modeling effort tractable, these results may be open to overinterpretation. Nevertheless, the model confirms the existence of a finite energy barrier for intershell transport, corroborating our experimental results.

Our DFT calculations were performed at the local density approximation [29] level of theory using the local orbital SIESTA code [30]. A double zeta plus polarization basis set was used in all calculations, and a Troullier–Martins type [31] norm-conserving nonlocal pseudopotentials were used to describe C in the [He] $2s^2 2p^2$ electronic configuration. The equilibrium atom positions were determined by requiring the forces on each atom to be $< 0.4 \text{ eV/nm}$. A schematic of the charge transport model is shown in Fig. 3(d).

IV. SUMMARY

In summary, at low electric fields carrier transport in multiwalled CNTs occurs primarily through thermal hopping of carriers across a $\sim 60\text{--}250 \text{ meV}$ energy barrier between individual shells in the same or adjacent CNTs. As the field increases the barrier decreases linearly with the square root of the electric field, causing superlinear $I\text{--}V$ behavior attributed to incremental field assisted intershell injection of charge carriers to the inner shells of the multiwalled CNT. $I\text{--}V$ characteristics at high fields follow the Poole–Frenkel charge transport model suggesting that cross-shell defects might play an important role

${}^2\Delta T = VIL/4\kappa A$ for one-dimensional thermal transport where V , I , L , κ , and A are the voltage, current, length, thermal conductivity (3000 W/m-K), and cross-section area of the CNT, respectively. Heat dissipation from the transverse surfaces of the CNT by conduction, convection, or radiation are neglected to consider a worst case scenario.

in intershell conduction. Intershell hopping of charge carriers is further confirmed by DFT calculations.

ACKNOWLEDGMENT

R. Ramprasad acknowledges the Institute of Materials Science (University of Connecticut) for providing the computational resources.

REFERENCES

- [1] Q. Ngo, D. Petranovic, S. Krishnan, A. M. Cassell, Q. Ye, J. Li, M. Meyyappan, and C. Y. Yang, "Electron transport through metal-multiwall carbon nanotube interfaces," *IEEE Trans. Nanotechnol.*, vol. 3, no. 2, pp. 311–317, Jun. 2004.
- [2] S. Frank, P. Poncharal, Z. L. Wang, and W. A. de Heer, "Carbon nanotube quantum resistors," *Science*, vol. 280, pp. 1744–1746, 1998.
- [3] M. S. Dresselhaus, G. Dresselhaus, and P. C. Eklund, *Science of Fullerenes and Carbon Nanotubes*. New York: Academic, 1996, pp. 802–803.
- [4] B. Q. Wei, R. Vajtai, Y. Jung, J. Ward, R. Zhang, G. Ramanath, and P. M. Ajayan, "Organized assembly of carbon nanotubes—Cunning refinements help to customize the architecture of nanotube structures," *Nature*, vol. 416, pp. 495–496, 2002.
- [5] S. Agrawal, M. J. Frederick, F. Lupo, P. Victor, O. Nalamasu, and G. Ramanath, "Directed growth and electrical-transport properties of carbon nanotube architectures on indium tin oxide films on silicon-based substrates," *Adv. Funct. Mater.*, vol. 15, pp. 1922–1926, 2005.
- [6] H. T. Ng, B. Chen, J. E. Koehne, A. M. Cassell, J. Li, J. Han, and M. Meyyappan, "Growth of carbon nanotubes: A combinatorial method to study the effects of catalysts and underlayers," *J. Phys. Chem. B*, vol. 107, pp. 8484–8489, 2003.
- [7] S. Agrawal, A. Kumar, M. J. Frederick, and G. Ramanath, "Hybrid architectures from aligned carbon nanotubes and silica particles," *Small*, vol. 1, pp. 823–826, 2005.
- [8] J. Li, Q. Ye, A. Cassell, H. T. Ng, R. Stevens, J. Han, and M. Meyyappan, "Bottom-up approach for carbon nanotube interconnects," *Appl. Phys. Lett.*, vol. 82, pp. 2491–2493, 2003.
- [9] P. Poncharal, C. Berger, Y. Yi, Z. L. Wang, and W. A. de Heer, "Room temperature ballistic conduction in carbon nanotubes," *J. Phys. Chem. B*, vol. 106, pp. 12104–12118, 2002.
- [10] M. Zamkov, N. Woody, B. Shan, Z. Chang, and P. Richard, "Lifetime of charge carriers in multiwalled carbon nanotubes," *Phys Rev Lett.*, vol. 94, p. 056803, 2005.
- [11] P. G. Collins, R. Martel, K. Liu, and P. Avouris, "Multiple shell diffusive conduction in multiwalled carbon nanotubes," in *AIP Conf. Proc.*, 2000, vol. 544, pp. 385–389.
- [12] B. Bourlon, C. Miko, L. Forro, D. C. Glattli, and A. Bachtold, "Determination of intershell conduction in multiwalled carbon nanotubes," *Phys. Rev. Lett.*, vol. 93, p. 176806, 2004.
- [13] A. Hansson and S. Stafstrom, "Electronic structure calculations of potassium-intercalated single-walled carbon nanotubes," *Phys. Rev. B*, vol. 67, p. 075406, 2003.
- [14] S. Roche, F. Triozon, A. Rubio, and D. Mayou, "Conduction mechanisms and magnetotransport in multiwalled carbon nanotubes," *Phys. Rev. B*, vol. 64, p. 121401, 2001.
- [15] S. Roche, F. Triozon, A. Rubio, and D. Mayou, "Electronic conduction in multi-walled carbon nanotubes: Role of intershell coupling and incommensurability," *Phys. Lett. A*, vol. 285, pp. 94–100, 2001.
- [16] P. G. Collins and P. Avouris, "Multishell conduction in multiwalled carbon nanotubes," *Appl. Phys. A*, vol. 74, pp. 329–332, 2002.
- [17] P. G. Collins, M. S. Arnold, and P. Avouris, "Engineering carbon nanotubes and nanotube circuits using electrical breakdown," *Science*, vol. 292, pp. 706–709, 2001.
- [18] P. G. Collins, M. Hersam, M. S. Arnold, R. Martel, and P. Avouris, "Current saturation and electrical breakdown in multiwalled carbon nanotubes," *Phys. Rev. Lett.*, vol. 86, pp. 3128–3131, 2001.
- [19] S. Agrawal, M. S. Raghuvver, H. Li, and G. Ramanath, "Defect-induced electrical conductivity increase in individual multiwalled carbon nanotubes," *Appl. Phys. Lett.*, vol. 90, p. 193104, 2007.
- [20] S. Agrawal, M. S. Raghuvver, R. Kroger, and G. Ramanath, "Electrical-current induced structural changes and chemical functionalization of carbon nanotubes," *J. Appl. Phys.*, vol. 100, p. 094314, 2006.
- [21] P. G. Collins and P. Avouris, "Intershell conductance of multiwalled carbon nanotubes," in *AIP Conf. Proc.*, 2002, vol. 633, pp. 223–226.

- [22] C. Miko, M. Milas, J. W. Seo, E. Couteau, N. Barisic, R. Gaal, and L. Forro, "Effect of electron irradiation on the electrical properties of fibers of aligned single-walled carbon nanotubes," *Appl. Phys. Lett.*, vol. 83, pp. 4622–4624, 2003.
- [23] C. Miko, M. Milas, J. W. Seo, R. Gaal, A. Kulik, and L. Forro, "Effect of ultraviolet irradiation on macroscopic single-walled carbon nanotube bundles," *Appl. Phys. Lett.*, vol. 88, p. 151905, 2006.
- [24] A. K. Dutta, "Electrical conductivity of single crystals of graphite," *Phys. Rev.*, vol. 90, pp. 187–193, 1953.
- [25] M. S. Raghuveer, P. G. Ganesan, J. D'Arcy-Gall, G. Ramanath, M. Marshall, and I. Petrov, "Nanomachining carbon nanotubes with ion beams," *Appl. Phys. Lett.*, vol. 84, pp. 4484–4486, 2004.
- [26] Z. Yao, C. L. Kane, and C. Dekker, "High-field electrical transport in single-wall carbon nanotubes," *Phys. Rev. Lett.*, vol. 84, pp. 2941–2944, 2000.
- [27] J. Frenkel, "On the theory of electric breakdown of dielectrics and electronic semiconductors," *Tech. Phys. USSR*, vol. 5, pp. 685–687, 1938.
- [28] J. Frenkel, "On pre-breakdown phenomena in insulators and electronic semiconductors," *Phys. Rev.*, vol. 54, pp. 647–648, 1938.
- [29] R. Martin, *Electronic Structure: Basic Theory and Practical Methods*. New York: Cambridge Univ. Press, 2004.
- [30] J. M. Soler, E. Artacho, J. Gale, A. Garcia, J. Junquera, P. Ordejon, and D. Sanchez-Portal, "The SIESTA method for ab initio order-N materials simulation," *J. Phys., Condens. Matter*, vol. 14, pp. 2745–2779, 2002.
- [31] N. Troullier and J. L. Martins, "Efficient pseudopotentials for plane-wave calculations," *Phys. Rev. B*, vol. 43, pp. 1993–2006, 1991.

Authors' photographs and biographies not available at the time of publication.